

## Tensile and high-cycle fatigue properties of spray formed Al10.8Zn2.9Mg1.9Cu alloys after two-stage aging treatment

WANG Zi-xing(王资兴)<sup>1,2</sup>, ZHANG Yong-an(张永安)<sup>1</sup>, ZHU Bao-hong(朱宝宏)<sup>1</sup>,  
LIU Hong-wei(刘红伟)<sup>1</sup>, WANG Feng(王 锋)<sup>1</sup>, XIONG Bai-qing(熊柏青)<sup>1</sup>

1. State Key Laboratory for Fabrication and Processing of Nonferrous Metals,  
General Research Institute for Nonferrous Metals, Beijing 100088, China;

2. School of Materials Science and Engineering, University of Science and Technology Beijing, Beijing 100083, China

Received 3 September 2005; accepted 6 March 2006

**Abstract:** Based on the investigation of the tensile properties of spray formed ultra-high strength Al10.8Zn2.9Mg1.9Cu alloys, the high-cycle fatigue properties under different theoretical stress concentration factors were investigated, the fatigue fracture surfaces and microstructures were observed, and the fatigue mechanism was discussed. The results indicate that the ultimate tensile strength of spray formed Al10.8Zn2.9Mg1.9Cu alloys can reach up to 730–740 MPa, and the elongation is about 8%–10% under the condition of two-stage aging treatment. For the stress ratio is 0.1, the maximum stress for  $10^7$  cycles is over 400 MPa and 120 MPa, when the theoretical stress concentration factor is 1 and 3, respectively.

**Key words:** Al10.8Zn2.9Mg1.9Cu alloy; spray forming; ultra-high strength aluminum alloy; high-cycle fatigue properties

### 1 Introduction

Ultra-high strength Al-Zn-Mg-Cu alloys have been widely used in the aerospace industry, traffic department and other areas because of high strength, light density and other excellent properties[1,2]. During the past decades, increased efforts have been made to improve the structural efficiency and properties of aerospace materials through the development of lighter mass, stiffer and stronger materials via rapid solidification processing[3,4]. Rapid solidification processing improves the mechanical properties by allowing higher solubility of the alloying elements while avoiding composition segregation and precipitate coarsening which are common in conventional ingot metallurgy technology.

Recently, the spray forming processing has attracted considerable attention as an alternative route for the synthesis of a variety of structural materials[5, 6]. This technique differs from conventional rapid solidification/power metallurgy(RS/PM) technology in which atomization and consolidation processes are combined in a single operation. The reduction in the number of manufacturing

steps can lead to significant economical savings. Furthermore, this process is carried out under an inert (typically nitrogen) atmosphere and therefore the brittle oxide content can be reduced and thus the ductility and fracture toughness can be improved. The latest investigations indicate that the Al-Zn-Mg-Cu alloys which are produced by spray forming could obtain good tensile properties after appropriate thermomechanical treatment and heat treatment [6–8].

However, high strength Al-Zn-Mg-Cu alloys are susceptible to intergranular stress corrosion cracking (SCC). Grain boundaries are often more susceptible to corrosion than the grain interiors because of the microstructural heterogeneity associated with the grain boundaries. The overaging treatment T7X has been applied to reduce the susceptibility of Al-Zn-Mg-Cu alloys to SCC which involves solution treatment followed by a two-stage aging treatment.

The objective of this study is to characterize the fatigue and fracture mechanics behavior of spray formed ultra-high strength Al10.8Zn2.9Mg1.9Cu alloys based on the investigation of the tensile properties with the aim of evaluating the critical variables affecting their damage tolerance properties.

## 2 Experimental

The nominal composition of the alloy was: 10.8%Zn, 2.86%Mg, 1.9%Cu, 0.16%Zr, 0.1%Ni (mass fraction) and balance aluminum. The spray-deposition experiments were conducted in SF-200 type environmental chamber. The as-deposited billets were machined to 124 mm in diameter and following a homogenizing treatment, they were hot-extruded at a temperature of 410 °C with a reduction ratio of 38:1 and a ram speed of 3 mm/s. In this study, the heat treatment for the alloy was as follows: the solution treating at 450 °C for 1 h and 475 °C for 1.5 h followed by water quenching, and two-stage artificial ageing for 16 h at 120 °C (T6) plus 4 h at 160 °C.

The tensile properties of the alloy were measured by MTS-810 test machine at a constant speed of 2 mm/min. The high-cycle fatigue experiments were performed by PLG-100C at room temperature with a stress ratio  $R$  of +0.1 at a frequency of 105–110 Hz, and the theoretical stress concentration( $K_t$ ) was 1 and 3. The fracture surfaces and the microstructures of the samples were carried out with CAMBRIDGE-2 scanning electron microscope, equipped with an energy dispersive spectrometer(EDS). The TEM studies were conducted on a JEM-2010 transmission electron microscope operated at an acceleration voltage of 200 kV.

## 3 Results and discussion

### 3.1 Tensile properties at room temperature

Tensile properties for the T6 and two-stage aging treatment are summarized in Table 1. It can be seen that the alloy fabricated by spray forming after hot extrusion and heat treatment can obtain high tensile properties: the ultimate tensile strength can reach up to 800–810 MPa and the elongation is 8%–10% at the T6 temper; the ultimate tensile strength is 730–740 MPa and the elongation is 8%–10% at the two-stage aging treatment.

**Table 1** Tensile properties of alloys at room temperature

| Aging     | YS/MPa  | UTS/MPa | Elongation/% |
|-----------|---------|---------|--------------|
| T6        | 780–790 | 800–810 | 8–10         |
| Two-stage | 710–720 | 730–740 | 8–10         |

The main causes that the alloy is able to obtain very high tensile properties at the two tempers can be summarized as follows:

Firstly, the optimizing chemical composition of the alloy. In this alloy, the Zn content reaches up to 10.8%, which is much higher than that of traditional Al-Zn-Mg-Cu alloys[8–10]. The higher Zn content and an appropriate value of the Zn/Mg lead to the increase of

the volume fraction of hardening precipitates (intermediate  $\eta'$  and equilibrium  $\eta$  ( $\text{MgZn}_2$ )), thus the tensile strength of the alloy is increased[11, 12].

Secondly, the refined and uniform microstructure of the alloy. During spray forming process, the cooling rate is very high which can reach up to  $10^3$ – $10^4$  °C/s[13], and the grains in the microstructure of as-deposited alloys are refined (the average size of the grains is about 20–30  $\mu\text{m}$ ). Moreover, due to the high cooling rate, the segregation of coarse phases is reduced; the size, shape and distribution of the second phase particles are also inclined to be uniform. These changes can contribute to the improvement of the properties of the alloy.

Thirdly, reasonable double-stage solution treatment. Under the double-stage solution treatment, the low-melting-point phases firstly dissolve to the matrix as much as possible, and high-melting-point phases will be dissolved in the second temperature stage, so the second phases will be dissolved on the whole. After later heat-treatment, the alloy can obtain high properties based on this condition.

Fig.1 shows the bright field TEM photograph of the alloy aged for 16 h at 120 °C(T6 temper). It can be seen that the precipitates are very small in size, and the grain boundary precipitates are continuous. After aging for 16 h at 120 °C plus 4 h at 160 °C, the formation of the narrow PFZ in regions adjacent to grain boundaries and local precipitation of small grain boundary particles are observed. In this case, the grain boundary precipitates are discontinuous (Fig.2). The discontinuous and growing grain boundary precipitates have been suggested to reduce the susceptibility to SCC by changing the slip planarity and hydrogen transport conditions[14, 15].

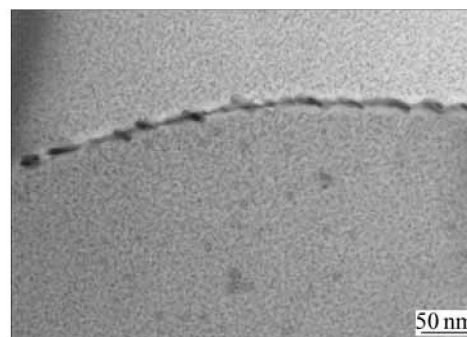


**Fig.1** TEM photograph of alloy aged for T6 temper

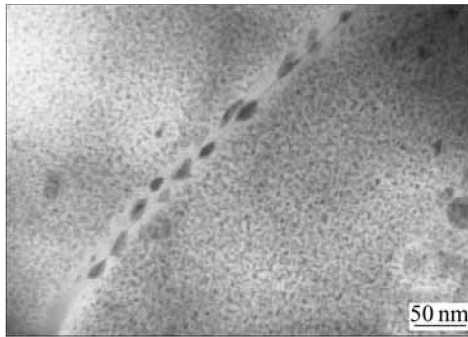
### 3.2 High-cycle fatigue properties

The high-cycle properties of the alloy at the two-stage aging treatment are shown in Table 2. For the stress ratio is 0.1, the maximum stress for  $10^7$  cycles is over 400 MPa and 120 MPa, when  $K_t$  is 1 and 3, respectively.

### 3.3 Mechanism of fatigue cracking propagation

**Table 2** High cycles properties of alloy at two-stage aging treatment

| Experimental condition | Maximum stress/MPa | Number of cycles/ $10^3$ |         |         |         |         |         |
|------------------------|--------------------|--------------------------|---------|---------|---------|---------|---------|
|                        |                    | 187                      | 860     | 270     | —       | —       | —       |
| $K_t=1$<br>$R=0.1$     | 450                | 187                      | 860     | 270     | —       | —       | —       |
|                        | 430                | 250                      | 79      | 72      | $>10^4$ | $>10^4$ | $>10^4$ |
|                        | 410                | $>10^4$                  | $>10^4$ | $>10^4$ | $>10^4$ | —       | —       |
| $K_t=3$<br>$R=0.1$     | 130                | 800                      | 336     | 1 186   | —       | —       | —       |
|                        | 125                | 3 850                    | 5 500   | 4 000   | $>10^4$ | $>10^4$ | $>10^4$ |
|                        | 120                | $>10^4$                  | $>10^4$ | $>10^4$ | —       | —       | —       |

**Fig.2** TEM photograph of alloy aged for two-stage aging treatment

The fatigue fracture morphologies of the samples at  $K_t=1$  are shown in Fig.3. The fracture surface is composed of fatigue source area, the first propagating area, the second propagating area, and the last cracking area. At the same time, evident shear lips can be observed. The whole fracture shape is similar to traditional ultra-high strength aluminum fatigue fracture [16].

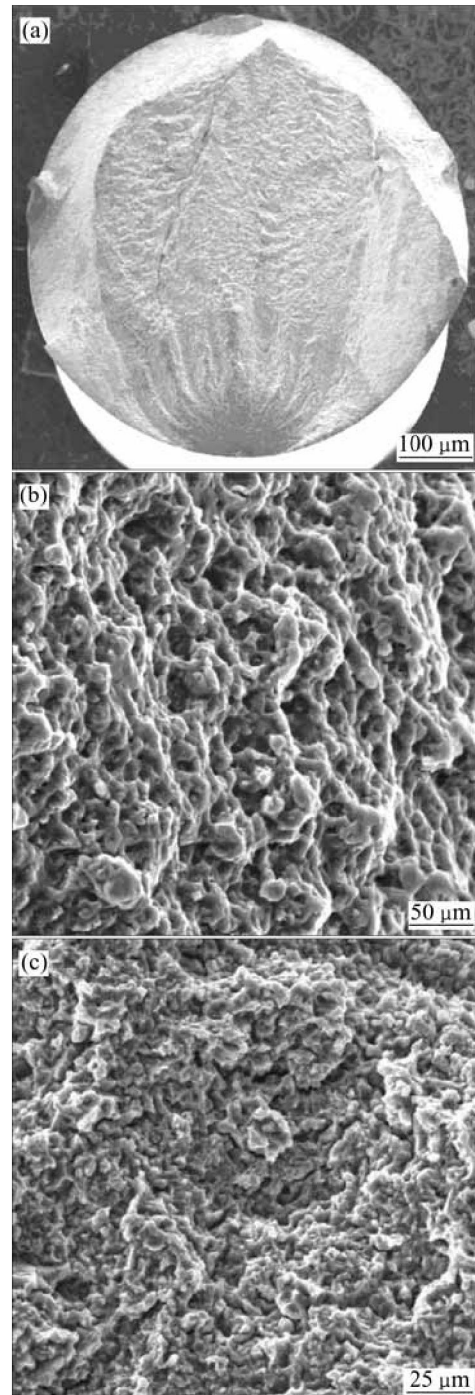
Moreover, with the observation of other samples at  $K_t=1$ , it is found that the fatigue source of each sample is single, and the mode of the propagation is two-stage: the initiation and the quicker propagation area. The former area is fan-like, and a lot of directionality dimples can be observed from high-magnification morphology (Fig.3(b)). In this area the cracking propagates slowly. In the second propagation area, a lot of shallow but no directionality dimples can be observed from high-magnification (Fig.3(c)), and the cracking propagates more quickly.

Fig.4 shows the fatigue fracture morphologies of the samples at  $K_t=3$ . The fracture surface is primarily composed of fatigue source area, the first propagating area and the second propagating area. The last cracking area and the shear lips are much smaller than the samples at  $K_t=1$ .

Moreover, with the observation of other samples at  $K_t=3$ , it is found that the number of the fatigue source of each sample is likely to be single, or to be multiple, as can be seen in Fig.4. The mode of the cracking propagation is also two-stage: the initiation area and the quicker propagation area.

### 3.4 Mechanism of fatigue crack initiation

The fatigue crack initiation sites of the specimens

**Fig.3** Fatigue fracture morphologies of samples at  $K_t=1$ : (a) Low-magnification morphology of fracture surface; (b) High-magnification morphology of first propagating area; (c) High-magnification morphology of second propagating area

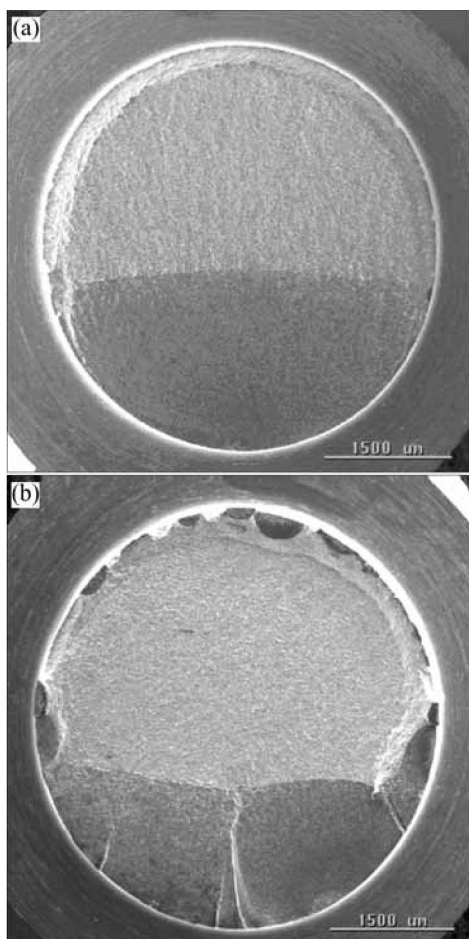


**Fig.4** Fatigue fracture morphologies of samples at  $K_t=3$ : (a) Single fatigue source sample; (b) Multiple fatigue sources sample

were investigated with scanning electron microscope and energy dispersive spectrometer(EDS) analysis. Combined with the microstructure analysis of the alloy, the result indicates that the fatigue crack initiations are inclined to begin at the coarse second phases, the microstructure defects and the machining exterior defects.

During the solution treating process, some of the second coarse phases which usually contain much Zn and Cu elements can not be dissolved to the matrix. The micro-crack is considered to be formed preferentially at the interfaces between the second phases and the matrix, where the stress concentration is more severe. Furthermore, the second phases are very brittle, and they are easily disconnected with the matrix or split as the fatigue stress acting on the specimens. Some of the micro-cracks generated from the second phases are found on the fatigue fracture surfaces, as can be seen in Fig.5.

Fig.6 shows that the cracking generates from the second phase. The EDS result of fatigue initiation area is shown in Table 3, the contents of Zn, Cu are much higher

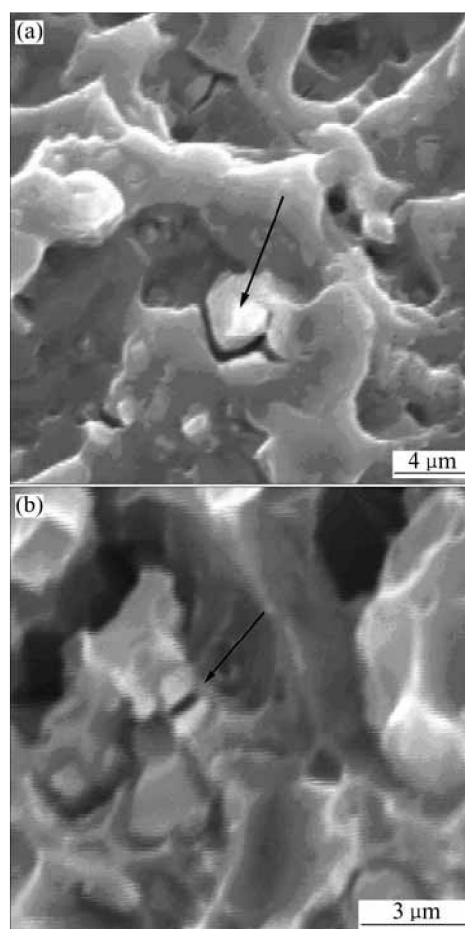


**Fig.5** Micro-cracks generated from second phases: (a) Second phase being disconnected with matrix; (b) Second phase being split by itself

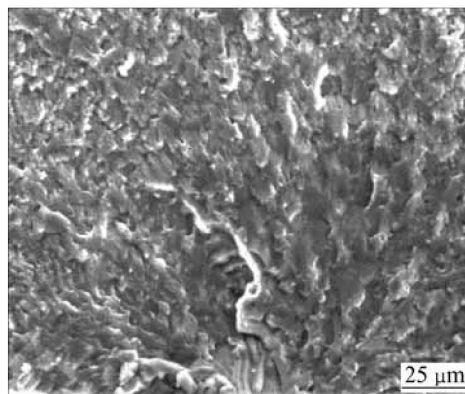


**Fig.6** Fatigue crack initiation from second phase

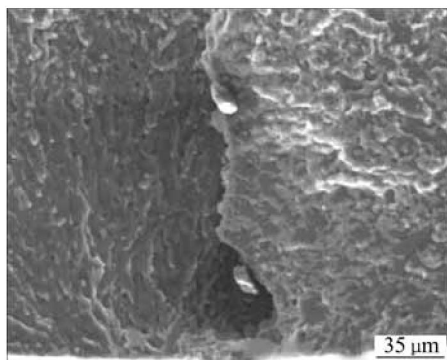
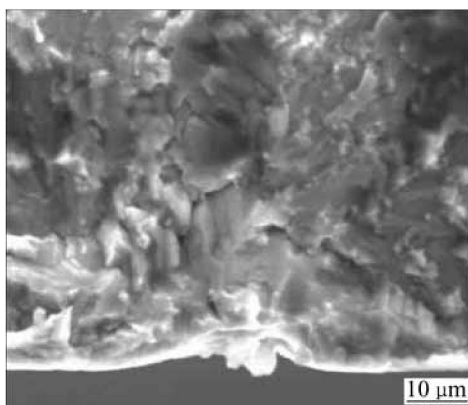
than the average contents of the alloy.

Fig.7 shows that the cracking generates from the material defect which is near the surfaces of the sample. This tiny microstructure defect can induce the stress concentration as the fatigue stress acting on the specimens, and then it may lead to a fatigue cracking source.

Fig.8 shows that the cracking generates from the

**Table 3** EDS result of fatigue initiation area (mass fraction, %)

| Zn   | Cu  | Mg  | Al   |
|------|-----|-----|------|
| 44.0 | 7.0 | 1.5 | 47.5 |

**Fig.7** Fatigue crack initiation from material defect**Fig.8** Fatigue crack initiation from machining defect

machining defect. With the observing of the samples, there are some tiny scratches on the surface. These machining defects can also induce stress concentration, so some of the tiny scratches may lead to a fatigue cracking source. The fatigue cracking initiation area turns to white because of the plastic deformation.

## 4 Conclusions

1) The ultimate tensile strength of spray formed Al10.8Zn2.9Mg1.9Cu alloys can reach up to 730–740 MPa and elongation is about 8%–10% under the condition of 16 h at 120 °C plus 4 h at 160 °C aging.

2) Spray formed Al10.8Zn2.9Mg1.9Cu alloy has excellent high-cycle fatigue properties under the condition of two stage aging treatment. For the stress ratio is 0.1, the maximum stress for  $10^7$  cycles is over 400 MPa and 120 MPa, when  $K_t$  is 1 and 3, respectively.

3) The mode of cracking propagation of spray formed Al10.8Zn2.9Mg1.9Cu alloy is a representative type of two-stage, and the fatigue crack initiations are inclined to begin at the coarse second phases, the microstructure defects and the machining exterior

defects.

## References

- [1] CHEN Chang-qi. Development of ultra-high strength aluminum alloys [J]. The Chinese Journal of Nonferrous Metals, 2002, 12(S): 22–27.(in Chinese)
- [2] POLMEAR I J. Aluminium alloys—a century of age hardening [A]. NIE J F, MORTON A J, MUDDLE B C, Proceedings of the 9th International Conference on Aluminium Alloys [C]. Australia: Institute of Materials Engineering Australasia Ltd, 2004: 1–14.
- [3] DUAN X M, HAO Y Y, YOSHIDA M, ANDO T, GRANT N J. Liquid dynamic composition of aluminum alloy 7150 [J]. The International Journal of Powder Metallurgy, 1993, 29(2): 149–160.
- [4] KUSUI J, FUJII K, YOKOE T, OSAMURA K, KUBOTA O, OKUDA H. Development of super-high strength AlZnMgCu P/M alloys [J]. Materials Science Forum, 1996, 217–222: 1823–1828.
- [5] BEFFORT O, SOLENTALER C, SPEIDEL M O. Improvement of strength and fracture toughness of a spray-deposited Al-Cu-Mg-Ag-Mn-Ti-Zr alloy by optimized heat treatments and thermomechanical treatments. Materials Science and Engineering A, 1995, 191(1): 113–120.
- [6] SHARMA M M, AMATEAU M F, EDEN T J. Mesoscopic structure control of spray formed high strength Al-Zn-Mg-Cu alloys [J]. Acta Materialia, 2005, 53(4): 2919–2924.
- [7] SANCTIS M D. Structure and properties of rapidly solidification ultra-high strength Al-Zn-Mg-Cu Alloys produced by spray deposition [J]. Materials Science and Engineering A, 1991, 141(1): 103–121.
- [8] ZHANG Yong-an, XIONG Bai-qing, ZHU Bao-hong, LIU Hong-wei, SHI Li-kai, WANG Hong-bin, ZHANG Ji-shan. Research on ultra-high strength Al10.8Zn2.9Mg1.7Cu alloys from spray forming [J]. Chinese Journal of Rare Metals, 2003, 27(5): 609–613.(in Chinese)
- [9] LIU Jing-an, XIE Shui-sheng. Application and Development of Aluminum Alloys [M]. Beijing: Metallurgical Industry Press, 2004: 101–104.(in Chinese)
- [10] WANG Zhu-tang, TIAN Rong-zhang. Aluminum Alloys Handbook [M]. Changsha: Central South University Press, 2000: 16–17.
- [11] ZHANG Yong-an. Research on Producing, Microstructures and Properties of Ultra-High Strength Aluminum Alloys from Spray Forming [D]. Beijing: General Research Institute for Nonferrous Metals, 2004.(in Chinese)
- [12] JUARE-ISLAS J A, PEREZ R, LENGSELD P, LAVERNIA E J. Microstructure and mechanical evaluations of sprayed-deposited 7XXX Al-alloys after conventional consolidation [J]. Materials Science and Engineering A, 1994(3): 614–618.
- [13] XU Q, LAVERNIA E J. Microstructure evolution during the initial stages of spray atomization and deposition [J]. Scripta Materials, 1999, 41(5): 535–540.
- [14] LIU Ji-hua. Effect of Heat Treatment on Stress Corrosion Cracking of 7075 Aluminum Alloy [D]. Beijing: Beijing University of Aeronautics and Astronautics, 2002.(in Chinese)
- [15] SONG Ren-guo, ZHANG Bao-jin, ZENG Mei-guang. The stress corrosion and role of Mg segregated to grain boundary in 7175 aluminium alloy [J]. Acta Metallurgica Sinica, 1997, 33(6): 595–601.
- [16] HOU Shu-e, DAI Li-jin, WANG Tian-zhong. Fatigue fracture behavior in smooth and notch specimens at different loads for an alloy LC9CGS3 [J]. Materials Engineering, 1996(1): 26–29.(in Chinese)

(Edited by LI Xiang-qun)